Journal of Biomechanical Engineering. Received April 23, 2010;
Accepted manuscript posted December 22, 2010. doi:10.1115/1.4003316

A Mathematical Simulation of the Ureter: Effects of the Model Parameters on Ureteral Pressure/Flow Relations

Bahman Vahidi[1], Nasser Fatouraee[1,*], Ali Imanparast[1], and Abbas Nasiraei Moghadam[1,2,3]

Bahman-Vahidi@aut.ac.ir, [*]Nasser@aut.ac.ir, A.Imanparast@aut.ac.ir, Abbas@caltech.edu

[1]Biological Fluid Mechanics Research Laboratory, Department of Biomedical Engineering, Amirkabir University of Technology (Tehran Polytechnic), Haafez Avenue, Tehran, Iran 15914

[2]Department of Radiology, Division of Diagnostic Cardiovascular Imaging, David Geffen School of Medicine at the University of California at Los Angeles, Los Angeles, California

[3]Department of Bioengineering, California Institute of Technology, Pasadena, California

[*]Phone: +98-2164542368

Fax: +98-21-666468186

WWW: http://bme.aut.ac.ir/Biofluids

Running Head: Mathematical Simulation of Ureter

Word count (including abstract+References+List of Figures and Tables):7305

Abstract

Ureteral peristaltic mechanism facilitates urine transport from the kidney to the bladder. Numerical analysis of the peristaltic flow in the ureter aims to further our understanding of the reflux phenomenon and other ureteral abnormalities. Fluid-structure interaction (FSI) plays an important role in accuracy of this approach and the Arbitrary Lagrangian-Eulerian (ALE) formulation is a strong method to analyze the coupled fluid-structure interaction between the compliant wall and the surrounding fluid. This formulation, however, was not used in previous studies of peristalsis in living organisms. In the present investigation, a numerical simulation is introduced and solved through ALE formulation to perform the ureteral flow and stress analysis. The incompressible Navier-Stokes equations are used as the governing equations for the fluid and a linear elastic model is utilized for the compliant wall. The wall stimulation is modeled by nonlinear contact analysis using a

rigid contact surface since an appropriate model for simulation of ureteral peristalsis needs to contain cell-to-cell wall stimulation. In contrast to previous studies, the wall displacements are not pre-determined in the presented model of this finite-length compliant tube, neither the peristalsis needs to be periodic. Moreover, the temporal changes of ureteral wall intraluminal shear stress during peristalsis are included in our study. Iterative computing of two-way coupling is used to solve the governing equations. Two phases of non-peristaltic and peristaltic transport of urine in the ureter are discussed. Results are obtained following an analysis of the effects of the ureteral wall compliance, pressure difference between the ureteral inlet and outlet, maximum height of the contraction wave, the contraction wave velocity and the number of contraction waves on the ureteral outlet flow. The results indicate that the proximal part of the ureter is prone to a higher shear stress during peristalsis compared to its middle and distal parts. It is also shown that the peristalsis is more efficient as the maximum height of the contraction wave increases. Finally, it is concluded that improper function of ureteropelvic junction results in the passage of part of urine back flow even in the case of slow start-up of the peristaltic contraction wave.

Keywords

Peristalsis, Vesicoureteral Reflux, Arbitrary Lagrangian-Eulerian formulation, FSI method.

Introduction

Peristaltic motion consists of successive sequence of contractions along a muscular tube. This motion is the driving force behind many critical functions in the human body such as transportation of urine from the kidney to the bladder. The mechanism that governs the ureteral peristalsis has been a focal point since the early beginning of peristaltic research [1]. Despite extensive research [1-3], this mechanism has not yet been fully understood, neither the pertaining mechanical factors have been analyzed precisely. For example the effects of ureteral wall compliance and inlet/outlet pressure differences on the peristaltic efficiency have not been accurately explained.

Stimulation of the ureter in peristalsis, creates a contraction wave that continuously travels, through a cell-to-cell propagation mechanism, from the site of stimulation to the bladder [4]. The passage of urine in the ureter can not be completely defined by peristaltic contractions. Indeed, it is known that the pressure difference between the renal pelvis and the bladder plays an observable role in the ureteral flow [3]. In a healthy ureter, ureteral peristalsis occurs only 1−5 times/min. When there is no peristaltic contraction (at the time intervals between two pace maker activations), the ureter can be seen as a passive tube that yields a steady flow of urine [2].

The irregular flow of urine from the bladder into the ureter, and possibly on to the kidneys is known as vesicoureteral reflux. In severe cases, vesicoureteral reflux may allow toxins and bacteria from the bladder to infect and hamper kidney function [3], thus leading to dialysis or in the critical cases, kidney transplantation [5].

A quantitative analysis to characterize urine flow will further aid our understanding of the ureter and also aid in the design of flow aided devices such as valves and stents to correct reflux conditions. The quantitative studies carried out in the field of experimental biomedicine up to now have been limited to 1) Urine volume transported, 2) Peristaltic wave propagation rate [8], 3) Morphometry of the ureter [9]. The qualitative studies in the biomedicine have also been focused on 1) Variations of ureteral lumen during peristalsis [10], 2) Reaction of the ureteral muscular tissue to drug and neurological stimulation [6,7,11-13], and 3) Different flow patterns occurring in the ureter [14-16] of various mammalians. Studies in the field of biomechanics have been concentrated on understanding the mechanical properties of the ureteral wall [17-20] and mathematical analyses of peristaltic flow to be applied to the gastro-intestinal system [21], the urinary system [3,22-25] and other living organs [26,27].

Due to the complexity of urine transport in the ureter, the recent mathematical simulations of the ureteral flow have also been restricted to very simple (2-D) geometries and boundary conditions [28-31].

The physiological function pertaining to the contraction rate of smooth muscle in the ureter is extremely complicated, and therefore, the ureteral smooth muscle has not yet been accurately modeled [32]. Three factors are identified as influencing the contraction rate of the ureteral smooth muscle: 1) the load against which the muscle is contracting (which largely consists of hydrodynamic (viscous) forces required to move urine,) 2) the current ureteral geometry, and 3) its state of activation.

Griffiths [33] published a theoretical analysis with numerical solutions evaluating the peristaltic flow through a distensible tube of limited length. The results showed that for flow with isolated boluses, the pressure/flow relation was determined by the active and passive properties of the tube undergoing peristalsis and not by the outlet load condition. The dynamics of the upper urinary tract and the effect of various bladder pressures on ureteral pressure/flow relations have also been studied by other researchers [2,15,16,24,28] but none of those studies included fluid-structure interaction in their analysis. Ureteral wall mechanical properties should not be over sighted in numerical analysis of ureteral function since they determine the significant deformations of ureteral wall, which play an important role in the urine transport from the kidney into the bladder. Wall deformations are caused by the wall stimulation as well as fluid forces, and therefore need to be studied through fluid-structure interaction. We should mention that in order to reach a reliable simulation, wall configuration should not be predetermined in the ureter during peristalsis because of the associated effects of wall compliance and fluid intraluminal pressure. To the best of our knowledge, this issue was not addressed in previous presented models of finite-length ureter.

We previously modeled a two-dimensional ureteral peristaltic flow [31] that assumed a solid wall moving along the longitudinal direction and between two rigid plates. The foremost shortcoming of that study was that the cell-to-cell stimulation of ureteral wall during peristalsis, which occurs in the physiological condition of ureteral peristalsis, was not modeled. Here, an axisymmetric non-linear FSI model is presented using real ureteral data. We aim to tackle the problem of ureteral peristaltic activity, taking in to account ureteral wall compliance and its cell-to-cell stimulation, in order to investigate the effects of different mechanical parameters on the ureteral flow and stress analysis that results in the better understanding of ureteral function. The main intents of this research are: 1) analyzing urine flow field in the ureter in order to better understand the reflux phenomenon, 2) quantitative analysis of peristaltic efficiency in different ureteral functional situations and 3) exploring the temporal changes in ureteral wall shear stress during the peristaltic wave propagation.

2. Materials and methods

The goal of this study is to improve the realism of computational solution of the problem of urine transport from the kidney into the bladder. Numerical simulation with fluid-structure interaction is presented. The computational analysis of a FSI problem requires two modeling steps: the creation of a mathematical-mechanical model and solving the coupled equations of the fluid and the structure.

2.1. Geometry of the model

The ureter was assumed to be like an axisymmetric tube. The ureteral diameter, including the muscular coat, varies from 4 to 10 mm [28]. In this study, it was assumed to be 9 mm. Figure 1 illustrates the geometry of the ureteral computational model. The rigid

contact surface shown in this figure, simulates a deformable wall stimulator that propagates the peristaltic wave through the ureter.

2.2. Governing equations

2.2.1. Fluid

A transient viscous flow in an axisymmetric tube (Fig.1.) was used to obtain desirable equation parameters. The incompressible Navier-Stokes equations were used as the governing equations with the assumptions of laminar and Newtonian flow. The continuity and momentum equations for the incompressible fluid, respectively, are:

$$\nabla . \boldsymbol{u} = \mathbf{0} \qquad (1)$$

$$\rho^f \frac{\partial u_i}{\partial t} + \rho^f \left(u_j - \frac{\partial d_j^f}{\partial t} \right) \frac{\partial u_i}{\partial x_j} = \frac{\partial \tau_{ij}^f}{\partial x_j} \qquad (2)$$

where $\boldsymbol{u}$ and u_i are the fluid velocity vector and the fluid velocity in the direction *i*, respectively, ρ^f is the fluid density, and d_j^f is the fluid displacement along the fluid-structure interface or other moving boundaries. The stress tensor can also be presented as shown below:

$$\tau_{ij}^f = -p\,\delta_{ij} + 2\mu e_{ij} \qquad (3)$$

where p is the fluid pressure, δ_{ij} is the Kronecker delta, and μ is the fluid viscosity. Fluid weight term was ignored in the equations. The strain tensor e_{ij} is defined as follows:

$$e_{ij} = \frac{1}{2}\left(\frac{\partial u_i}{\partial x_j} + \frac{\partial u_j}{\partial x_i} \right) \qquad (4)$$

where u_i and u_j are the fluid velocities in the directions i and j, respectively.

2.2.2. Solid

The ureteral wall is modeled mathematically utilizing the classical Lagrangian formulation, which is as follows:

$$\frac{\partial \tau_{ij}^{s}}{\partial x_j} = \rho^{s} \frac{\partial^2 d_i^{s}}{\partial t^2} \qquad (5)$$

where τ_{ij}^{s} is the Cauchy stress tensor, d_i^{s} is the solid displacement component and ρ^{s} is the solid density.

2.2.3. Fluid-Structure Interaction

In this formulation, the coupling state of the fluid and the structure interaction must be satisfied. The kinematic coupling conditions, which represent the no-slip conditions at the interface, are:

$$d_i^{f} = d_i^{s} \qquad (6a)$$

$$\frac{\partial d_i^{f}}{\partial t} = \frac{\partial d_i^{s}}{\partial t} \qquad (6b)$$

The above equations require that the values of displacement and velocity for both the fluid and the solid be the same at the interface boundary.

The kinetic coupling condition shows the equilibrium of forces as given below:

$$n_j \tau_{ij}^{f} = n_j \tau_{ij}^{s} \qquad (7)$$

where *n* is the unit vector normal to the interface of the fluid and solid regions. Eq. (7) provides the balance of forces between the fluid and the structure at the interface boundary.

2.3. Materials properties and boundary conditions

2.3.1. Fluid

The urine in the ureter was assumed to be homogenous with a constant density of ρ=1050 kg/m^3 and viscosity of μ=1.3 cP. The boundary conditions for the fluid regions are:

(1) No slipping takes place between the fluid and the ureteral wall and that no penetration of the fluid through the ureteral wall occurs, (2) A pressure difference between the outlet and the inlet of the ureter is needed to perform the flow in the non-peristaltic transport of urine. This pressure difference varies between -0.05 Pa and 0.3 Pa in different numerical models (the pressure magnitudes applied to the ureteral inlet and outlet can be seen in Table 1), (3) FSI conditions are defined between the ureteral wall and urine on their interface all through the model.

2.3.2. Solid

Material properties for the wall were assumed to be linear elastic, isotropic, incompressible and homogeneous with two different Young modulus of E=5 kPa and 10 kPa that were approximated from the stress/stretch relations reported by Yin and Fung [20] from their experimental studies on the ureteral tissue. The boundary conditions for the wall were: (1) The wall was fixed at the inlet and outlet in the longitudinal direction to prevent rigid body motion error in the finite element model. (2) It was assumed that a rigid contact surface mechanically stimulates a deformable wall (Fig. 1.). When the solution reaches the steady state with the correct velocity profile and the right pressure drop along the ureter (t=12 s), the rigid contact surface moves in the axial direction along the ureter with a constant velocity (1 to 2 cm/s) similar to that which exits in the physiological ureteral peristalsis [22,28] to model the ureteral peristaltic flow, (3) As for the fluid model, FSI conditions were defined between the ureteral wall and urine.

2.4. Simulation process

Discretization changes the form of the partial differential equations to algebraic equations, and therefore facilitates the numerical solution of the equations. Computational

fluid dynamics (CFD) uses numerical methods and algorithms to solve fluid flow problems using the discretized form of Newton's Second Law. For various coupled problems, the fluid traction affects the solid's deformations while the structural displacement affects the flow field. This verity is the reason to accomplish fluid-structure interaction analyses. In this study, ADINA software (v8.5, ADINA R&D, Inc., Watertown, MA), which uses the Lagrangian formulation in the structural model and the Arbitrary Lagrangian–Eulerian (ALE) formulation in the fluid counterpart, was employed to solve the fully coupled system. The governing equations of the fluid were solved utilizing upwind scheme, finite element methods and sparse solver (which employs the standard Galerkin method for incompressible fluid flow). The Euler and Implicit-Newmark integration methods were used for the fluid and the solid, respectively. An iterative Newtonian method was used for solving the obtained weak form of the governing equations of the fluid and the structure. The number of iterations and iteration tolerance of velocity for the solid equations were set to 300 and 0.01, respectively. As for the fluid equations, these parameters were assumed to be 500 and 0.001, respectively, for a reliable convergence. Using direct computing of two-way coupling, the solution obtained was fully coupled and the kinematical conditions of displacement, velocity, and acceleration continuity across the no-slip fluid-solid (ureter-urine) interface were satisfied at all the time steps during the analysis.

2.5. Computational grid generation

Fluid domain was meshed with 54990 2-D Fluid axisymmetric type elements. All fluid elements were triangular and contained 3 nodes. 12960 2-D Solid axisymmetric type elements were used for the solid region. The whole solid elements were quadrilateral and contained 9 nodes. The quantity of the elements (referred above) for the fluid and solid

models were achieved by gradually increasing the number of elements until the solution became independent from the grid size. The typical refined mesh is shown in Fig. 1. The maximum solution time for the models was about 22 h on a 1.8 GHz Xeon Dual Core Intel (0.768 GB RAM) Processor.

3. Results

In this paper, a more proper mechanical model was presented compared to previous studies. The main benefit of this model is that multi functional factors that are essential in the ureteral performance were considered together. Moreover, ureteral muscular contraction was modeled using an external barrier. This method of stimulation imposes the least restrictions on ureteral dilatation. Dynamic interaction between urine and the ureteral wall during peristalsis was deliberated.

3.1. Flow Field and wall shear stress

The numerical model was solved for two different peristaltic velocities to obtain the ureteral outlet flow rate. The flow rates were measured at the end of the ureteral peristaltic motion or propagation wave. The velocity data at the ureteral outlet was integrated to compute the ureteral outlet flow rate.

Figure 2 shows the pressure profile in the ureter during the peristaltic wave propagation. As can be seen from this figure, there is an adverse pressure gradient occurred following the contraction wave peak. This undesired pressure gradient caused the recirculation regions in that area. By analyzing the pressure profiles at different times during peristalsis, it was determined that the adverse pressure gradient near the contraction wave peak, moved steadily along with the longitudinal propagation of the wave. This adverse pressure gradient created a

backward flow in the opposite direction of the peristaltic wave motion that can be verified by the fluid velocity vectors (Fig. 3). In this plot, the length of the vectors shows the relative urine velocity magnitude. Figure 3 illustrates the backward flow development at the beginning of peristalsis when the contraction wave was entering the ureter. Only a short time after the wave start-up, the backward flow occurs around the wave so that it affects the ureteral entrance. The physical reason for this event is the effect of the inertial forces suddenly applied to urine flow owing to the wall stimulation. As the wave propagated toward the ureter, a chronic back flow developed completely, which moved downstream along with the contraction wave propagation (Fig. 3-c) and the amounts of back flow at the ureteral inlet gradually diminished; so ureteropelvic reflux is more probable to be present at the beginning of the wall peristaltic motion.

The results showed that the pressure gradient magnitude along the ureteral longitudinal direction on its wall and symmetry line was the maximum value around the peak of the propagating contraction wave and these values decreased as a result of the wave dissemination in the longitudinal direction to the bladder, as is illustrated in Fig. 4.

The results also indicated that the wall shear stress near the peak of the moving contraction wave was the maximum. This stress decreased gradually by the peristaltic wave propagation toward the bladder (Fig. 5).

3.2. Effect of different parameters on the ureteral outlet flow rate

3.2.1. The ureteral wall compliance

To understand the effect of the ureteral wall compliance on the urine flow rate in the non-peristaltic mechanism, two numerical experiments were performed on the finite element model. In these experiments, a Young modulus of 5 and 10 kPa was utilized, which is in the

physiological range of human ureteral elasticity [20]. As predicted, ureteral wall dilatation with a wall Young modulus of 5 kPa was greater than that of the 10 kPa, so there was an increase in the ureteral internal diameter, resulting from the imposed pressure (the ureteral average pressure was supposed to be 130 Pa). With the assumption of *h* being constant, the decrease in ureteral wall elasticity results in higher dilatation of the ureter, and therefore, fluid volume transported by the peristaltic wave and consequently the ureteral outlet flow rate are expected to increase. This expectation was completely verified by all our numerical results. For instance, the difference between the ureteral diametrical expansions in two cases with different wall Young moduli can be seen from the ureteral outlet velocity magnitude profile in Fig. 6 and can be related to the different corresponding flow rate magnitudes. From this figure, ureteral dilatation difference at the radius of 3.5 mm is about 0.13 mm. The results indicate that the increase of ureteral wall compliance (decrease in ureteral wall Young modulus), accordingly enhances the urine transportation capacity in the ureter.

In order to determine how much the wall compliance affects the ureteral outlet flow rate in the non-peristaltic and peristaltic mechanisms of urine transportation, we increased the wall elasticity up to 1 GPa, which minimizes the effect of wall compliance on flow and preserves the dynamic wall configuration like the other FSI models undergoing peristalsis, that is needed for a true comparison between the models. The results shown in Fig. 6 illustrate the noticeable effect of wall compliance on urine flow in the non-peristaltic mechanism and the results related to peristaltic mechanism will be presented in 3.2.4.

3.2.2. The peristaltic wave velocity

Figure 7 shows urine velocity profile at the ureteral outlet for two different cases in which only the peristaltic wave velocity varies from 1 to 2 cm/s, at t=12 s (peristaltic wave

starting time) and at the end of the wall peristaltic activity in each model. Figure 7 also illustrates the condition in which the contraction wave moves with a low velocity magnitude. This motion does not have a considerable effect on the urine velocity magnitude; therefore, in these cases the peristaltic mechanism does not have a noticeable effect on the ureteral outlet flow rate. Thus the peristaltic efficiency is negligible. However, a contraction wave with a higher velocity (more than 1 cm/s) has a significant effect on the ureteral outlet flow rate.

3.2.3. Ureteral outlet and inlet pressure difference

In order to understand the effect of the peristaltic wave motion on the urine flow rate (peristaltic efficiency), one method is varying the ureteral inlet and outlet pressure and detecting the urine flow rate in the ureter, applying wall peristaltic motion. This situation was modeled with the assumption of 3 pressure differences (+0.3, 0, -0.05 Pa) between the ureteral inlet and outlet (The assumed pressure magnitudes which were applied to the ureteral inlet and outlet in different models can be seen in Table 1.). The effect of the pressure difference between the ureteral inlet and outlet on the urine flow rate at the ureteral outlet for different maximum heights of contraction waves is given in Table 1. For a better comparison, the ureteral outlet flow rate was calculated considering peristalsis and without wall peristaltic activity (at t=12 s, before the peristalsis start-up) and can be seen in Table1 and Fig. 8. Our results show that the urine flow rate increased by the peristaltic wave propagation up to 3 times the non-peristaltic flow (which can be simply calculated from the values given in Table1 and Fig. 8).

3.2.4. The maximum height of contraction wave

Figure 8 illustrates the relations between the ureteral flow rate, wall elasticity and the maximum height of the contraction wave as a result of the ureteral peristaltic activity. As

illustrated in Fig. 8, the ureteral outlet flow rate and hence the peristaltic efficiency increased by increasing the maximum height of the contraction wave. This occurred owing to a greater force being applied to the running fluid because of a greater constriction in the ureteral lumen as a result of wall stimulation.

The bilateral effects of the wall elasticity and the maximum height of the contraction wave on the flow rate are also illustrated in Fig. 8. Wall rigidity effects have also been considered in this study assuming E=1 GPa in order to determine how much wall compliance affects the urine flow via peristalsis, which can be seen in this figure. The lower magnitudes of flow rate in this figure relate to E=1 GPa in which the flow rate increases up to 13.9% by increasing *h* from 1.12 to 1.68, while in E=10 kPa and E=5 kPa, the flow rate increases up to 59.1% and 57.3%, respectively. Flow increases between 57.1% (the difference between E=1 GPa and E=10 kPa in *h*=1.12) up to 160% (the difference between E=1 GPa and E=5 kPa in *h*=1.68). As a consequence, the reduction of wall elasticity causes a greater flow rate in different values of the maximum height of the contraction wave but not in a linear pattern.

3.2.5. Effect of the simultaneous number of contraction waves

One of the major factors analyzed in this paper is the effect of a number of simultaneous wave contractions in the ureter and its effect on the ureteral outlet flow rate. In order to simulate this situation, the second rigid surface, which is the inducer of the second contraction wave, was moved from the same coordinate by the same velocity along the ureter with 5 s delay. The results of the flow rate taken from the ureteral outlet are presented in Fig.9. In Figure 9, the data of one contraction wave is also presented for comparison. The following items have been considered in each solution: 1) The moment of peristalsis start-up (t=12 s) and 2) the overall solution time that lasts during t=0 up to t=26 s including the time

interval of non-peristaltic phase in all of the models as well as the time interval in the model of one contraction wave, and at last, the time interval in the models of two simultaneous contraction waves during peristalsis with a delay of 5 s between the two successive contraction waves. It is obvious from the Fig. 9, a greater volume of urine per unit time is transported in the ureter in the model having one peristaltic wave than in the models having two simultaneous propagating contraction waves. Also, by the further propagation of the second wave in the ureter, the outlet flow rate decreases more.

4. Discussion

In general, four types of flow regimes were reported to occur in the ureter through peristalsis; they are isolated-bolus, boluses in contact, leaky-bolus and open-tube flow [15,16,33]. This study is limited to the open-tube flow regime which has the highest flow rate among aforementioned regimes. Also, the simulation is restricted to the condition in which the pressure difference between the renal pelvis and the bladder is insignificant.

After a thorough analysis of the flow field results (Fig. 3), it was concluded that ureteropelvic junction (UPJ) dysfunction (as modeled in this paper) results in the retrograde flow of urine even when there is a slow (not accelerated) start-up of the contraction wave. The reduction in the pressure gradient magnitude during the peristaltic wave propagation (Fig. 4) is due to the spontaneous acceleration of the fluid around the contraction wave and the subsequent immediate phase of urine deceleration, which is a result of the wave longitudinal propagation.

The ureteral wall stress results (Fig. 5) indicated that the maximum values of shear stress around the peak of the wave decreased by the wave longitudinal propagation, so it can be concluded that the proximal portion of the ureter, which is near the kidney, is prone to a

higher shear stress during the ureteral peristaltic mechanism. High values of shear stress at the beginning of the ureteral peristaltic activity is due to the spontaneous acceleration of the urine, which results in a large relative velocity difference between the urine near the wall (at the position of the contraction wave) and the whole urine in the ureter. This noticeable difference reduces gradually by the wave longitudinal propagation.

For the non-peristaltic mechanism of urine transport via the ureter (Fig. 6) considering the fact that the ureteral outlet flow rate is proportional to its diameter, we can manipulate the effect of the diametrical parameter by variation of two factors: 1) At the same wall compliance, assuming different diametrical values and 2) At the same geometrical condition (the equivalent diameters), assuming different compliance for the ureteral wall. In the latter situation, an increase in wall compliance (reduction of Young modulus) increases the ureteral wall dilatation and therefore results in flow rate increase.

For the effect of the peristaltic wave velocity on ureteral outlet flow rate (Fig. 7), it can be concluded that on every occasion that the velocity of the contraction wave is a low magnitude comparing to the time scale of fluid motion, the condition is so that the fluid does not sense the contraction wave movement and the contraction wave plays the role of a stenosis in the ureter, which leads to the increase of the ureteral resistance, that results in the decrease of ureteral outlet flow rate.

The obtained results regarding peristaltic efficiency are in good agreement with theory as well as previously published studies [29,34]. In particular the results pertaining to the maximum height of contraction wave (Fig. 8) are in accordance with findings of Carew and Pedley [34]. Making use of a mathematical simulation, they demonstrated that the constriction of the ureteral lumen during peristalsis has a major effect on peristaltic efficiency. They proved that the ureteral peristaltic pumping is most efficient in the case of a

ureter whose lumen can theoretically be pressed shut. Walker and Shelly [29] using a variational method for optimizing the shape of a peristaltic wave, reported that peristaltic flux increases by increasing the amount of occlusion in a 2-D channel. These findings were confirmed by our results in Fig. 8. They also showed that flux increases linearly by the occlusion. This result does not agree with our numerical results presented in Fig. 8. The contradiction seems to be due to adding the wall compliance in our models. It is illustrated in Fig. 8 that as the height of the contraction wave becomes smaller, the effect of wall elasticity on the urine flow rate decreases comparing E=5 kPa with E=10 kPa. The reason is that the situation is approaching to the completely open-tube condition, where the moving obstruction in the ureter is negligible and therefore, the peristaltic efficiency is near zero. By increasing the maximum height of the contraction wave, the effect of wall elasticity on the urine flow rate increases, although in cases of nearly complete occlusion of the ureteral lumen during peristalsis, the effect of wall elasticity on the urine flow rate (the difference between the magnitudes of flow rates in Fig. 8) decreases because of the dominant effect of fluid high pressure gradients around the peak of the propagating contraction wave. The noticeable effect of wall compliance on urine flow through peristalsis can be concluded comparing the magnitudes of flow rate in E=1 GPa (which minimizes the effect of wall compliance on flow) with E=5 kPa and E=10 kPa (which are in the physiological range of ureteral wall elasticity).

The simultaneous contraction waves and their effect on the ureter of pigs and humans have been investigated by biological experimentalists [2,15,16]. As it can be understood from Fig. 9 and because of the fact that contraction waves locally restrict the flow around the peak of the wave (the lumen area decreases), the reason for flow rate reduction in the models with two simultaneous contraction waves is the greater pressure drop along the ureter. This greater pressure drop is caused by the presence of two moving constrictions compared to one moving

constriction in the model with one contraction wave. In other words, despite enhancement of the urine flow propelling force by two contraction waves, the adverse effect of a pressure drop along the ureter is dominant, and thus an overall flow rate reduction occurs.

The results revealed a significant role of fluid-structure interaction on flow and stress analysis within a uniform compliant tube undergoing peristalsis. Similar to other models that simulate a system as sophisticated as a living organism, we made some simplifications in our approach. These simplifications were mostly in geometry and material properties. Mean physiological values from Yin and Fung [20] have been used for ureteral wall material properties. The ureteral wall was assumed to be straight, linearly elastic, homogeneous, and isotropic. Clearly, mammalian ureters exhibit wide variations in terms of shape, size, material properties, and loading conditions. Carew and Pedley [34] considered the viscoelastic properties of ureteral wall based on the reasonable assumption of the thin shell theory. However, their studies, which models periodic activation waves (a non-realistic biological assumption because of time independency of the equations in the wave frame) in an infinite tube, did not account for cell-to-cell stimulation of ureteral wall that describes the physiological conditions of peristaltic wave longitudinal propagation.

In addition to aforementioned complications regarding the geometry and material properties, there were also some difficulties pertaining to stability of the solutions of FSI equations. These difficulties mainly relate to the loading conditions of the ureteral wall in the FSI model. Since in this approach the interactions between urine and the ureter are also taken into account, the complications in each of the fluid and solid models are even more pronounced. With this in mind, it is essential to reduce uncertainties in the fluid and solid models prior to introduction of wall motion to the model that was sensitively satisfied in this study.

We assumed a fixed-velocity for the movement of the wall stimulator, i.e. the average velocity of peristalsis [22,28], which allows for peristaltic wave propagation through the ureter. It should be noted that in this paper, we did not consider the physiological conditions of ureter undergoing higher luminal pressure level, which varies between 20 to 40 mmHg in healthy ureters [28], due to computational restrictions, although by applying pressure loadings to the ureteral inlet and outlet, we assumed approximately the true constant level of pressure in the ureter that is between 1 to 6 mmHg [28]. In the physiological function of ureteral peristalsis, the contraction force generated by the smooth muscle depends on the luminal pressure [1]. Therefore, the prescribed radial fixation of the mechanical stimulator (rigid surface) during peristalsis in our model is another limitation which makes the maximum constriction independent of luminal pressure. The assumed axisymmetric geometry of the ureter model with uniform thickness is highly idealized and was performed to simplify the case so that the solution will be numerically tractable. More complicated shapes are required to model realistic ureteral dilatation due to the stellate form of the ureteral luminal area [10]. Such shapes will require the spatial finite element discretizations. Nonetheless, we should emphasize that the goal of the present work was not to model an isolated urine bolus movement in the ureter, but rather to develop a mathematical framework suitable for simulating the ureteral peristalsis. The use of mechanical stimulation to induce peristalsis, in the ureteral wall is novel and has not been previously addressed in the literature.

4.1. Future studies

There are still many unsolved problems in this field to which the introduced approach can be applied. For example, the complicated nature of reflux and the meaning of several diagnostic indicators are not well understood. The direct interaction between the two parts of

the urinary system (kidney and bladder) has scarcely received any theoretical contemplation. Furthermore, the wall activation by a pacemaker that induces peristalsis and the detailed process of the elastic deformation in the ureteral muscle which is highly nonlinear has not been fully explained.

The introduced model needs some improvements in future works to get closer to reality. For highly deformable ureteral wall, non-linear hyperelastic and viscoelastic models might represent ureteral wall more realistically. The aspects of initial stress and strain have not been incorporated in our proposed models yet, although their effects are not expected to invalidate the results of this study. The assumption of a time-dependent peristaltic velocity based on *in vivo* data, also results in a more realistic simulation and should be considered in future studies.

The modeling introduced in this paper may also be used to study the effect of non-Newtonian fluids on peristaltic pumping, which was investigated by Teran et al., [30] with 2-D models using immersed boundary method. Moreover, the non-return action of the ureterovesical junction (UVJ), which prevents the back flow from the bladder into the ureter, is an important phenomenon that can be simulated and better understood by our presented approach. Patient-specific modeling of ureteral mechanics based on geometric data using dynamic MRI or CT imaging will be valuable to identify crucial disease conditions.

5. Conclusions

In the present paper, a numerical simulation with fluid-structure interaction (FSI) for urine transport in the ureter was performed. This simulation introduces a new approach to evaluate more accurately the peristaltic mechanism in the ureter. The effect of physiological factors that influence the efficiency of the peristaltic process was investigated. These factors

include the pressure difference between the kidney and the bladder, ureteral wall compliance, peristaltic wave velocity, maximum height of the contraction wave, and the number of contraction waves, that affect the peristaltic efficiency, ureteral wall shear stress and the urine flow field. Our results indicated that there is a high possibility of occurrence of reflux at the beginning of peristalsis in the ureter. Moreover, the peristaltic efficiency is highly dependent on the ureteral wall compliance, and therefore, fluid-structure interaction plays an important role in analyzing the ureteral fluid dynamics.

References

[1] Fung, Y. C., 1971, ‘‘Peristaltic pumping: a bioengineering model, in: Boyarsky, S. Gottschalk, G. W., Tanagho, E. A., et al., eds., Urodynamics: Hydrodynamics of the Ureter and Renal Pelvis,’’ New York: Academic press, pp. 189-198.

[2] Griffiths, D. J., Constantinou, E. C., et al., 1987, ‘‘Dynamics of the upper urinary tract: II. The effect of variations of peristaltic frequency and bladder pressure on pyeloureteral pressure/flow relations,’’ Phys. Med. Biol., **32**(7), pp. 823-833.

[3] Bykova, A. A., Regirer, S. A., 2005, ‘‘Mathematical models in urinary system Mechanics,’’ Review article, J. Fluid Mech., **40**(1), pp. 221-226.

[4] Uehara, Y., Burnstock, G., 1970, ‘‘Demonstration of ‘‘gap junctions’’ between smooth muscle cells,’’ J Cell Biol., **44**, pp. 215-217.

[5] Eccles, M. R., 1998, ‘‘The role of PAX2 in normal and abnormal development of the urinary tract,’’ Pediatr. Nephrol., **12**, pp. 712-720.

[6] Kontani, H., Ginkawa, M., Sakai, T., 1993, ‘‘A simple method for measurement of ureteric peristaltic function in vivo and the effects of drugs acting on ion channels applied from the ureter lumen in anesthetized rats,’’ Jpn. J. Pharmacol., **62**, pp. 331-338.

[7] Jorgensen, T. M., 1986, ‘‘Pathogenetic factors in vesicoureteral reflux,’’ Neurourol. Urodynam., **5**, pp. 153-183.

[8] Saeki, H., Morita, T., et al., 1985, ‘‘Changes in the ureteral peristaltic rate and the bolus volume in gradual and rapid urinary flow increase,’’ Tohoku J. Exp. Med., **146**, pp. 273-275.

[9] Zelenko, N., Coll, D., et al., 2004, ‘‘Normal ureter size on unenhanced helical CT,’’ Am. J. Roentgenol., **182**, pp. 1039-1041.

[10] Woodburne, R. T., Lapides, J., 1972, ‘‘The ureteral lumen during peristalsis,’’ Am. J. Anat., **133**(3), pp. 255-258.

[11] Liu, J. X., Park, Y. C., et al., 1991, ''Ureteral perfusion in normal and chronically obstructed feline models,'' Korean J Urol., **32**(6), pp. 980-985.

[12] Mahoney, Z. X., Sammut, B., et al., 2006, ''Discs-large homolog 1 regulates smooth muscle orientation in the mouse ureter,'' Proc. Natl. Acad. Sci. U.S.A., **103**(52), pp. 19872-19877.

[13] Aragona, F., Artibani, W., et al., 1988, ''The morphological basis of ureteral peristalsis,'' Int. Urol. Nephrol., **20**(3), pp. 239-250.

[14] Melchior, H., 1975, ''Urodynamics,'' Urol. Res., **3**, pp. 51-54.

[15] Ohlson, L., 1989, ''Morphological dynamics of ureteral transport I. Shape and volume of constituent urine fractions,'' Am. J. Physiol., **256**, pp. R19-R28.

[16] Ohlson, L., 1989, ''Morphological dynamics of ureteral transport II. Peristaltic patterns in relation to flow rate,'' Am. J. Physiol., **256**, pp. R29-R34.

[17] Fung, Y. C., 1993, ''Biomechanics: Mechanical properties of living tissues,'' Springer-Verlag, New York.

[18] Hansen, I., Gregersen, H., 1999, ''Morphometry and residual strain in porcine ureter,'' Scand. J. Urol. Nephrol., **33**, pp. 10-16.

[19] Knudsen, L., Gregersen, H., et al., 1994, ''Elastic wall properties and collagen content in the ureter: an experimental study in pigs,'' Neurourol. Urodynam., **13**, pp. 597-608.

[20] Yin, F. C. P., Fung, Y. C., 1971, ''Mechanical properties of isolated mammalian ureteral segments,'' Am. J. Physiol., **221**(5), pp. 1484-1493.

[21] Gregersen, H., Kassab, G., 1996, ''Biomechanics of the gastro-intestinal tract,'' Review article. Neurogastroenterol. Motil., **8**, pp. 277-297.

[22] Gintz, D., Elmabsout, B., Renaudeaux, J. P., 1999, ''Modelling of the urine flow in the human ureter,'' C. R. Acad. Sci. Paris, **t. 327**, Seri II b, pp. 1265-1268.

[23] Gintz, D., Elmabsout, B., Renaudeaux, J. P., 2001, ''Modelling of the human ureteral bolus,'' C. R. Acad. Sci. Paris, **t. 329**, Seri II b, pp. 303-306.

[24] Griffiths, D. J., Notschaele, C., 1983, ''The mechanics of urine transport in the upper urinary tract: the dynamics of the isolated bolus,'' Neurourol. Urodynam., **2**, pp. 155-156.

[25] Vogel, A., Elmabsout, B., Gintz, D., 2004, ''Modelling of urine flow in a ureteral bolus,'' C. R. Mecanique, **332**, pp. 737-742.

[26] Eytan, O., Jaffa, A. J., Elad, D., 2001, ''Peristaltic flow in a tapered channel: application to embryo transport within the uterine cavity,'' Med. Eng. Phys., **23**, pp. 473-482.

[27] Misra, J. C., Pandey, S. K., 2001, ''A mathematical model for oesophageal swallowing of a food-bolus,'' Math. Comput. Model., **33**, pp. 997-1009.

[28] Jiménez-Lozano, J., 2009, ''Peristaltic flow with application to ureteral Biomechanics,'' PhD. Thesis in Mechanical Engineering, Notre Dame University, Indiana, USA.

[29] Walker, S. W., Shelley, M. J., 2010, ''Shape optimization of peristaltic pumping,'' J. Comput. Phys., 229, PP. 1260-1291.

[30] Teran, J., Fauci, L., Shelley, M. J., 2008, ''Peristaltic pumping and irreversibility of a Stokesian viscoelastic fluid,'' Phys. Fluids., **20**, PP. 073101-1 - 073101-11.

[31] Vahidi, B., Fatouraee, N., 2007, ‘‘Mathematical modeling of the ureteral peristaltic flow with fluid structure interaction,’’ J. Biomech., **40**, Supplement 2, p. S223.

[32] Bykova, A. A., Regirer, S. A., 1999, ‘‘Simple model of peristalsis in a myogenically-active tube,’’ Euromech. Colloquium, **389**, Book of abstracts, Graz, pp. 68-69.

[33] Griffiths, D. J., 1987, ‘‘Dynamics of the upper urinary tract: I. Peristaltic flow through a distensible tube of limited length,’’ Phys. Med. Biol., **32**(7), pp. 813-822.

[34] Carew, E. O., Pedley, T. J., 1997, ‘‘An active membrane model for peristaltic pumping. Pt 1. Periodic activation waves in an infinite tube,’’ J. Biomech. Eng., **119**(1), pp. 66-76.

Captions

Figure 1. FSI computational model. As it is shown, the rigid contact surface motion leads to contraction wave propagation in the ureter. *h* reperesents the maximum height of contraction wave. The model is axisymmetric, although the complete model is presented here for better illustration.

Figure 2. Ureteral pressure profile during peristaltic wave propagation. The results are related to the case of E = 5 kPa, V = 2 cm/s, h = 1.68 mm, Δp = 0.3 Pa. The pressure profile is relatively similar around the contraction wave peak during all the solution time.

Figure 3. Urine velocity vector plot showing ureteral back flow development following the contraction wave at the beginning of peristalsis. In this plot, time is considered from the beginning of peristalsis and the length of the vectors shows the relative velocity magnitude; (a) The contraction wave is entering into the ureter, the urine flow field varies slightly, (b) A moderate back flow is developing at the ureteral entrance, (c) A chronic back flow has been developed completely, which moves along with the contraction wave propagation downstream.

Figure 4. Pressure gradient magnitude; (a) along the ureteral wall, (b) along the ureteral symmetry line; the results are related to the case of E = 5 kPa, V = 2 cm/s, h = 1.4 mm, Δp = 0.3 Pa. Times shown on the figure were measured from the beginning of peristalsis.

Figure 5. Shear stress on the ureteral wall in the case of E = 5 kPa, V = 2 cm/s, h = 1.4 mm, Δp = 0.3 Pa. Times shown on the figure were measured from the beginning of peristalsis. This pattern of shear stress reduction was observed in all the numerical experiments.

Figure 6. Urine velocity magnitude versus the distance from the ureteral axis at the ureteral outlet in the case of non-peristaltic flow for two numerical experiments with Δp = 0.3 Pa, and different Young modulus of E = 5 kPa, E = 10 kPa, and E = 1 GPa.

Figure 7. Urine velocity magnitude versus the distance from the ureteral axis at the ureteral outlet for two numerical experiments with different peristaltic velocities of V = 1 cm/s and V = 2 cm/s. The curves shown in this figure relate to non-peristaltic flow at t = 12 s (the peristaltic wave beginning moment) and to the end of the wall peristaltic activity when the wave reaches the ureter outlet. The Effect of peristalsis on urine velocity can be seen from the figure obviously. The related parameters are: E = 5 kPa, h = 1.68 mm, Δp = 0.3 Pa.

Figure 8. Urine flow rate versus the maximum height of the contraction wave for three numerical experiments with different Young modulus of E = 5 kPa, E = 10 kPa, and E= 1GPa. The related parameters are: V = 2 cm/s, Δp = 0.3 Pa.

Figure 9. Urine flow rate at the ureteral outlet during peristalsis. This figure shows the effect of the number of contraction waves on the amount of urine transported in the ureter. The moment of peristalsis start-up is at t = 12 s and the overall solution time lasts during t = 0 up to t = 26 s including the time interval of non-peristaltic phase in all of the models as well as the time interval in the model of one contraction wave, and at last, the time interval in the models of two simultaneous contraction waves during peristalsis with a delay of 5 s between the two successive contraction waves. The related parameters are: E = 5 kPa, V = 2 cm/s, h = 1.68 mm, Δp = 0.3 Pa.

Table 1. Effect of pressure difference between the ureteral inlet and outlet on the urine flow rate at the ureteral outlet in the models with different maximum heights of contraction waves. In these cases, the ureteral Young modulus and the contraction wave velocity were assumed to be 5 kPa and 2 cm/s, respectively.

Journal of Biomechanical Engineering. Received April 23, 2010;
Accepted manuscript posted December 22, 2010. doi:10.1115/1.4003316

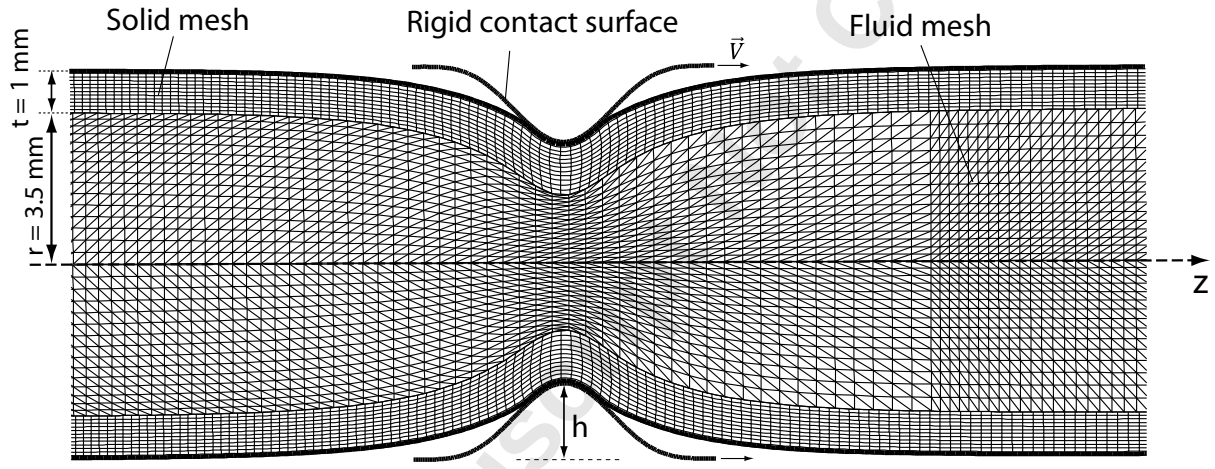

Figure 1. FSI computational model. As it is shown, the rigid contact surface motion leads to contraction wave propagation in the ureter. *h* reperesents the maximum height of contraction wave. The model is axisymmetric, although the complete model is presented here for better illustration.

Journal of Biomechanical Engineering. Received April 23, 2010;
Accepted manuscript posted December 22, 2010. doi:10.1115/1.4003316

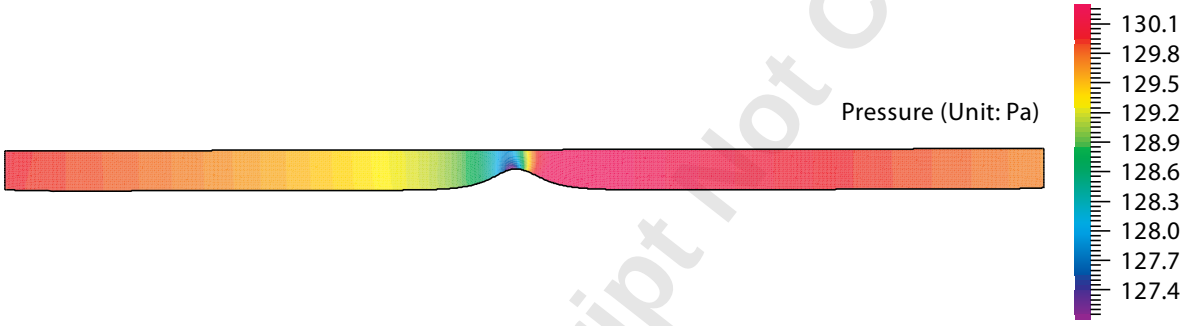

Figure 2. Ureteral pressure profile during peristaltic wave propagation. The results are related to the case of E = 5 kPa, V = 2 cm/s, h = 1.68 mm, Δp = 0.3 Pa. The pressure profile is relatively similar around the contraction wave peak during all the solution time.

Journal of Biomechanical Engineering. Received April 23, 2010;
Accepted manuscript posted December 22, 2010. doi:10.1115/1.4003316

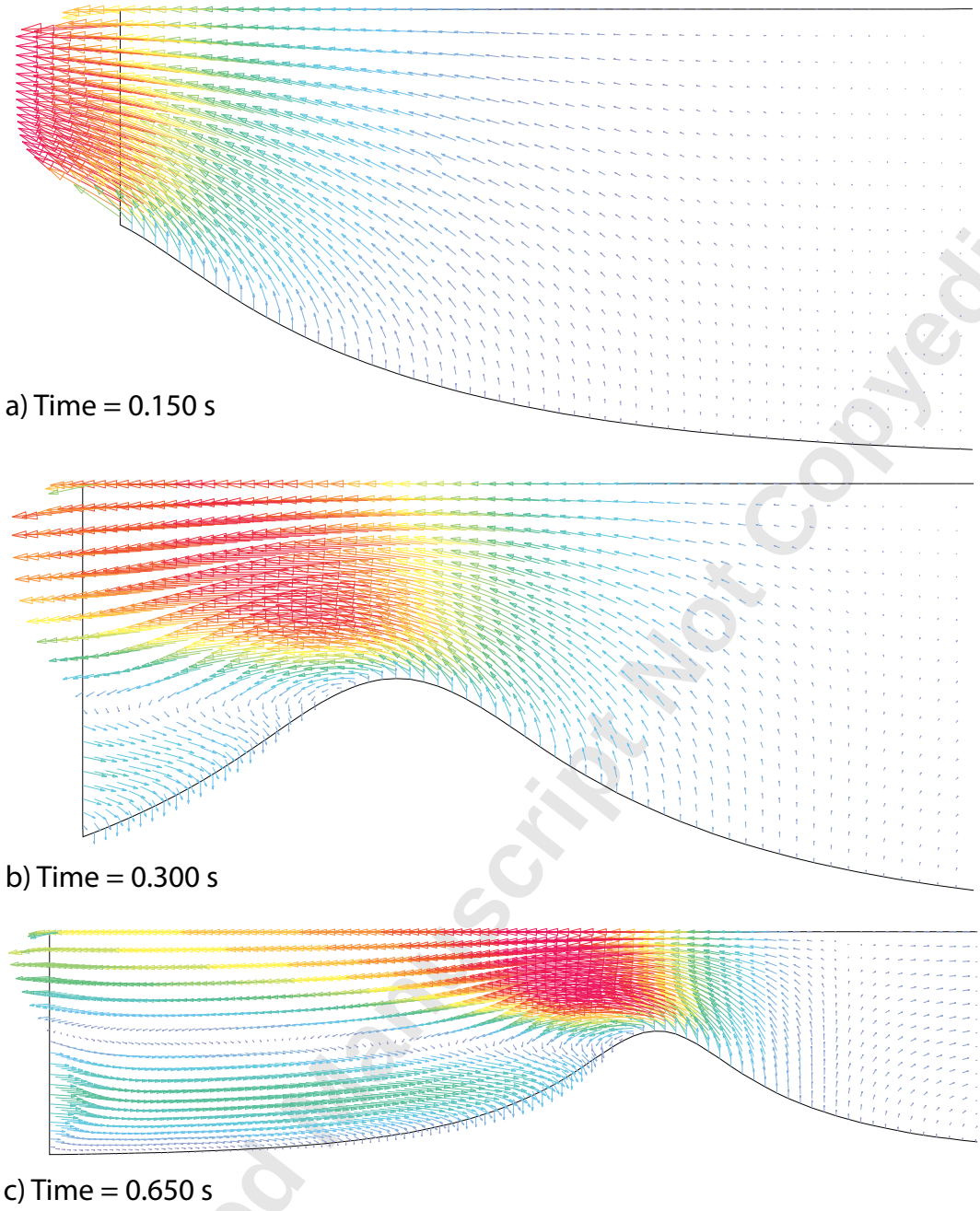

Figure 3. Urine velocity vector plot showing ureteral back flow development following the contraction wave at the beginning of peristalsis. In this plot, time is considered from the beginning of peristalsis and the length of the vectors shows the relative velocity magnitude; (a) The contraction wave is entering into the ureter, the urine flow field varies slightly, (b) A moderate back flow is developing at the ureteral entrance, (c) A chronic back flow has been developed completely, which moves along with the contraction wave propagation downstream.

Journal of Biomechanical Engineering. Received April 23, 2010;
Accepted manuscript posted December 22, 2010. doi:10.1115/1.4003316

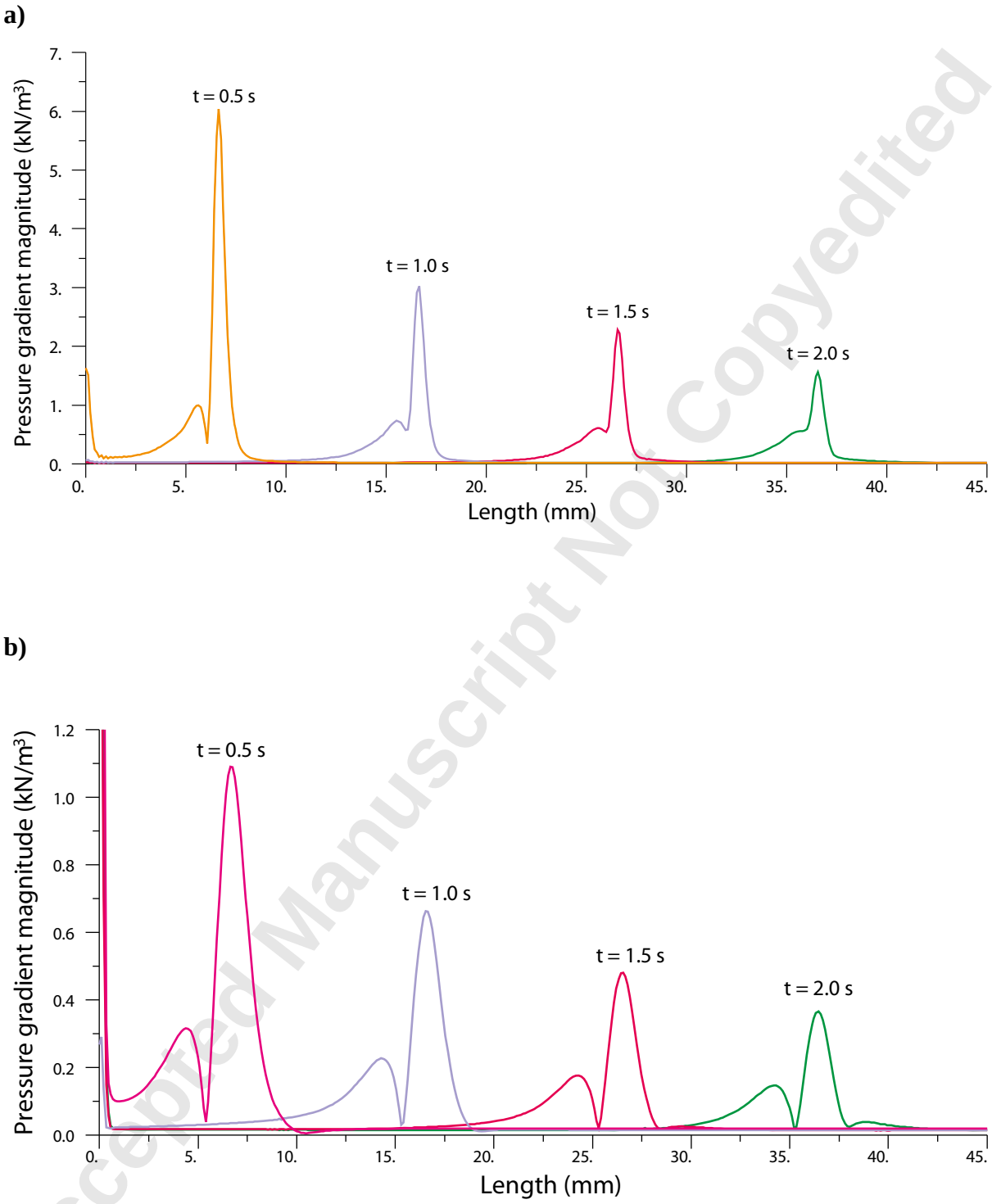

Figure 4. Pressure gradient magnitude; (a) along the ureteral wall, (b) along the ureteral symmetry line; the results are related to the case of E = 5 kPa, V = 2 cm/s, h = 1.4 mm, Δp = 0.3 Pa. Times shown on the figure were measured from the beginning of peristalsis.

Journal of Biomechanical Engineering. Received April 23, 2010;
Accepted manuscript posted December 22, 2010. doi:10.1115/1.4003316

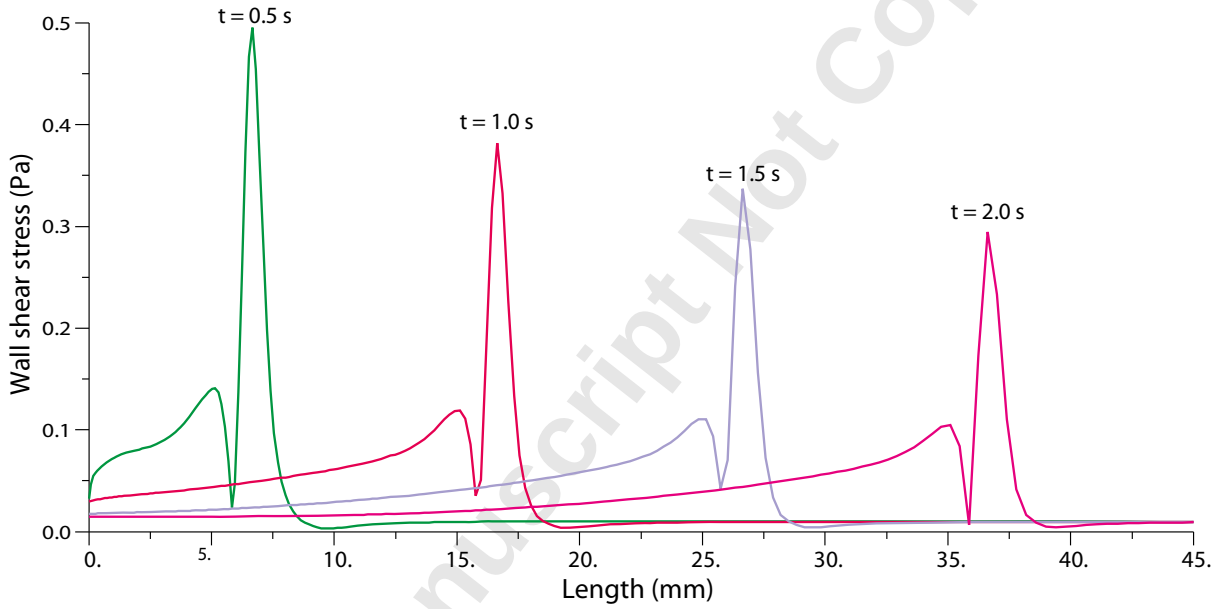

Figure 5. Shear stress on the ureteral wall in the case of E = 5 kPa, V = 2 cm/s, h = 1.4 mm, Δp = 0.3 Pa. Times shown on the figure were measured from the beginning of peristalsis. This pattern of shear stress reduction was observed in all the numerical experiments.

Journal of Biomechanical Engineering. Received April 23, 2010;
Accepted manuscript posted December 22, 2010. doi:10.1115/1.4003316

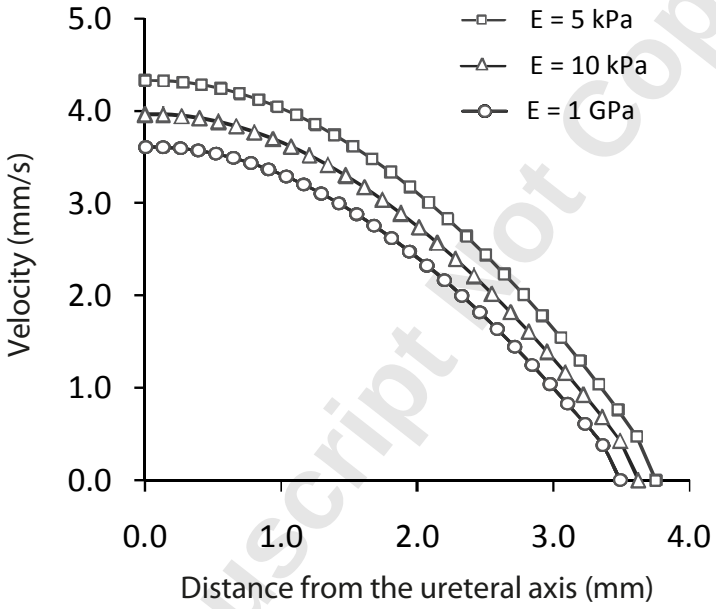

Figure 6. Urine velocity magnitude versus the distance from the ureteral axis at the ureteral outlet in the case of non-peristaltic flow for two numerical experiments with $\Delta p = 0.3$ Pa, and different Young modulus of E = 5 kPa, E = 10 kPa, and E = 1 GPa.

Journal of Biomechanical Engineering. Received April 23, 2010;
Accepted manuscript posted December 22, 2010. doi:10.1115/1.4003316

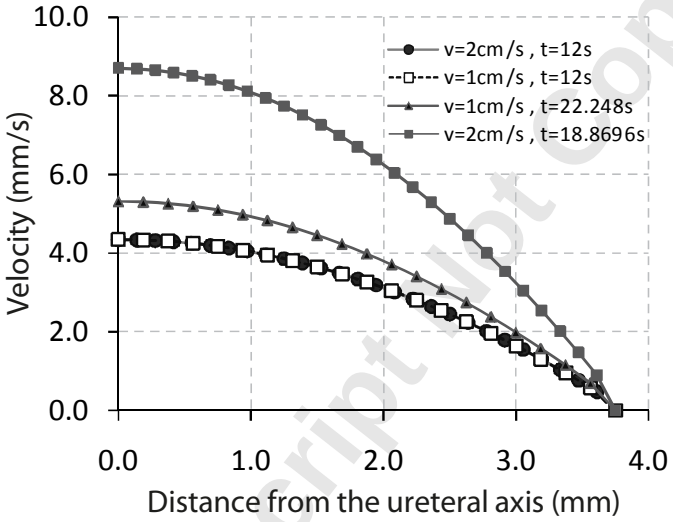

Figure 7. Urine velocity magnitude versus the distance from the ureteral axis at the ureteral outlet for two numerical experiments with different peristaltic velocities of V = 1 cm/s and V = 2 cm/s. The curves shown in this figure relate to non-peristaltic flow at t = 12 s (the peristaltic wave beginning moment) and to the end of the wall peristaltic activity when the wave reaches the ureter outlet. The Effect of peristalsis on urine velocity can be seen from the figure obviously. The related parameters are: E = 5 kPa, h = 1.68 mm, Δp = 0.3 Pa.

Journal of Biomechanical Engineering. Received April 23, 2010;
Accepted manuscript posted December 22, 2010. doi:10.1115/1.4003316

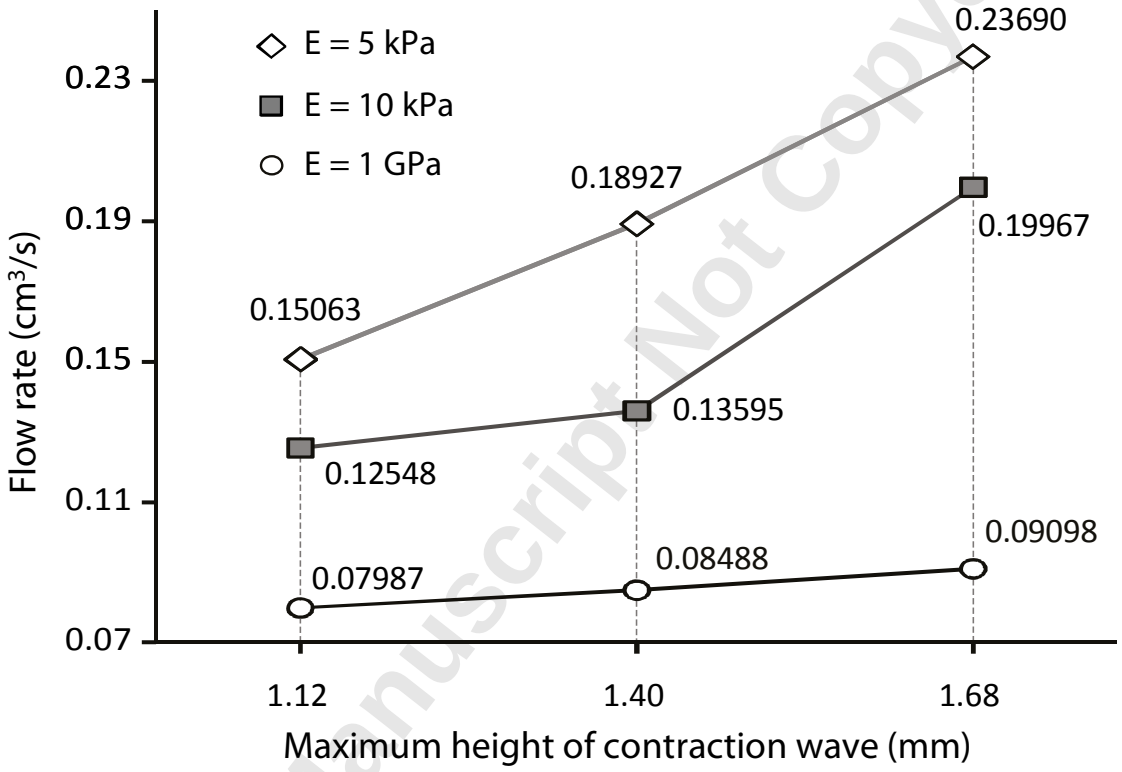

Figure 8. Urine flow rate versus the maximum height of the contraction wave for three numerical experiments with different Young modulus of E = 5 kPa, E = 10 kPa, and E= 1GPa. The related parameters are: V = 2 cm/s, Δp = 0.3 Pa.

Journal of Biomechanical Engineering. Received April 23, 2010;
Accepted manuscript posted December 22, 2010. doi:10.1115/1.4003316

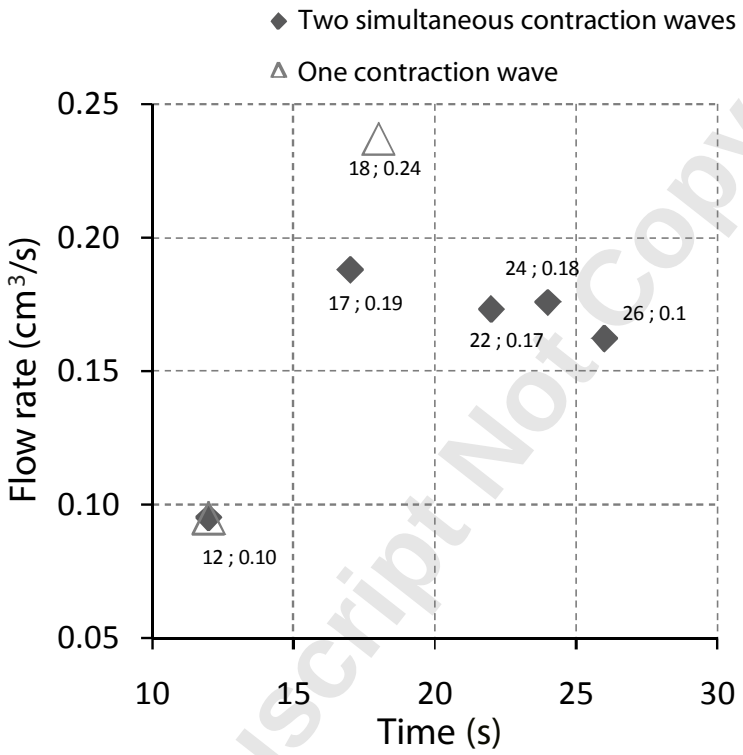

Figure 9. Urine flow rate at the ureteral outlet during peristalsis. This figure shows the effect of the number of contraction waves on the amount of urine transported in the ureter. The moment of peristalsis start-up is at t = 12 s and the overall solution time lasts during t = 0 up to t = 26 s including the time interval of non-peristaltic phase in all of the models as well as the time interval in the model of one contraction wave, and at last, the time interval in the models of two simultaneous contraction waves during peristalsis with a delay of 5 s between the two successive contraction waves. The related parameters are: E = 5 kPa, V = 2 cm/s, h = 1.68 mm, Δp = 0.3 Pa.

Journal of Biomechanical Engineering. Received April 23, 2010;
Accepted manuscript posted December 22, 2010. doi:10.1115/1.4003316

Table 1. Effect of pressure difference between the ureteral inlet and outlet on the urine flow rate at the ureteral outlet in the models with different maximum heights of contraction waves. In these cases, the ureteral Young modulus and the contraction wave velocity were assumed to be 5 kPa and 2 cm/s, respectively.

Maximum height of contraction wave (mm)	**Ureteral outlet pressure (Pa)**	**Ureteral inlet pressure (Pa)**	**Ureteral pressure difference between its outlet and inlet (Pa)**	**Flow rate difference between t=12 s (peristaltic wave starting time) and the ending time of wall peristaltic motion at the ureteral outlet (cm^3/s)**
1.4	**129.7**	**130**	**+0.3**	**9.4183×10^{-2}**
1.68	**129.7**	**130**	**+0.3**	**1.4204×10^{-1}**
1.4	**130**	**130**	**0**	**1.3831×10^{-1}**
1.68	**130**	**130**	**0**	**1.9745×10^{-1}**
1.4	**130**	**129.95**	**-0.05**	**1.4523×10^{-1}**
1.68	**130**	**129.95**	**-0.05**	**2.0987×10^{-1}**